Exploration on visualization for an interactive 3D map for mineralogy distribution on the lunar surface

MSc thesis

Christina Irakleous

Universiteit Leiden

Exploration on visualization for an interactive 3D map for mineralogy distribution on the lunar surface

A thesis submitted in partial fulfillment
of the requirements for the degree of

Master of Science

in

Creative Intelligence and Technology (Media Technology)

Author:	Christina Irakleous
Student ID:	s3729664
Supervisor:	Prof. Dr. Ir. F. J. Verbeek
Second supervisor:	Fatemeh Fazel Hesar

Cover image: View of Schroeter's Valley and crater Aristarchus photographed by Apollo 15, NASA ID: S71-44666

Universiteit Leiden

P.O. Box 9513, 2300 RA Leiden, The Netherlands

Abstract

This project explores the development of an interactive 3D visualization tool based on lunar observations and machine learning (ML) analysis, combining data from remote sensing imaging and spectroscopy. Data visualization is an important tool for analysis and for science communication, especially in the field of planetary surface exploration. Building an interactive 3D map -compared to the static maps that already exist- is a novel tool for data analysis regarding the comparison of the spectral and mineralogical characteristics of the lunar surface. Based on ML plots, new global maps can provide more accurate visualization regarding mineral abundances, results that can be used to build a scientific tool for per pixel analysis and further mineral comparison. For the Moon multiple missions provided various datasets of spectroscopy, and they are available on-line on NASA and ESA platforms. This study investigates the Aristarchus crater, one of the largest craters with olivine observations. Applying principles from human-centered design, the objective is to create a scientific tool and investigate if interactive 3D data visualization can enhance the analysis of machine learning results in lunar mineralogy with comparison to the 2D outputs. Early testing shows promising results, as the 3D version revealed spatial correlations with spectral data and improved users' understanding of mineralogical distribution compared to the 2D version.

Acknowledgements

First and foremost, I would like to express my deepest gratitude to my supervisors, Prof. Fons Verbeek and Fatemeh Fazel Hesar. Their guidance, encouragement, and support were essential for the completion of this thesis. I am also very grateful to Prof. Bernard Foing for his inspiration and advice and to Dr. Chrysa Avdelidou and Dr. Mojtaba Raouf for kindly serving as critics of my work. I would like to thank Dr. Megha Bhatt who gave us their datasets and her permission to use them for the purpose of this thesis. I also thank the 15 participants for their time to contribute to this project and my friend Antonis Theodorakakos for his valuable suggestions.

Beyond academia, I owe special thanks to my friends Katerina and Kallinikos for their help when I arrived in the Netherlands. I am equally grateful to my closest friends, Vaso, Tre and Eva, as well as my cousin Nikoleta and my friend Evi, who had no idea what I was doing for my research, but were always there to listen. I would also like to thank Dr. Nick Samaras for his valuable help and Prof. Thanasis Economou and Aristeidis Voulgaris for their support. From Media Technology, a special thanks also goes to Emma, Annelies, Nikki and Yanna, my partners in crime in this master's.

Lastly, I would like to thank my dog, Pixel. Pixel patiently waited for me to return from the University, stayed by my side while I was studying for every course, and kept me company. For his devotion, I would like to dedicate this thesis to my dog, Pixel.

Contents

1. Introduction

1.1 Background

Data visualization plays a crucial role in modern science, both for science communication and research. However, the need to visualize what we observe is not a novel thing. Visualization has its roots in early cave drawings, since humanity began to observe the world around us and for the need of communication. From Leonardo da Vinci's scientific illustrations to the computer revolution, data visualization has become an important tool over the years with applications in many domains such as medicine, engineering and science (Brodbeck et al., 2009).

Today, in fields like astronomy and space exploration, where datasets are large and expanding daily, visualization becomes the bridge between the numbers and the human interpretation (Dykes et al., 2018). Visualization in astronomy can be used for many purposes (Hassan and Fluke, 2011) and we can classify the astronomical visualization in five data tasks: data wrangling, data exploration, feature identification, object reconstruction, and outreach (Lan et al., 2021).

In planetary science, visualization is an essential tool and is commonly used for planetary mapping. Remote sensing missions scan our solar system, collecting data from the planets, satellites, and smaller bodies. The purpose of remote sensing missions is to study the mineralogy, geology, and resource potential of our terrestrial neighborhood. The Moon was one of the first bodies to be observed and studied. Its exploration is important because it can provide useful insights regarding the early Earth-Moon system, terrestrial planet differentiation and evolution, the solar system impact record, and the lunar environment in general (National Research Council, 2007).

These missions collect extensive datasets, both topographic and spectroscopic, allowing us to reconstruct the lunar surface with great detail. Spectroscopic observations of the Moon focus mostly on mineral distribution. Spectroscopy is very important for lunar exploration, and extensive research has been done on it over the last few years (Wu and Hapke, 2018; Thoresen et al., 2024; Thapa et al., 2025). All of these spectroscopic datasets are being processed today with the help of multiple machine learning techniques, mostly to classify mineral types and estimate the abundances of the minerals. Thus, there are a great number of existing studies that depict 2D static maps of the Moon or regions of the Moon, usually depicting the mineralogical abundances with false colors.

1.2 Research Gap

VR and AR have been used extensively by NASA and ESA, combining principles from Human-Computer Interaction (HCI) in space exploration (Olbrich et al., 2018) . Space agencies use emerging technologies in cases such as digital twins and simulation, training, operations support, psychological countermeasures in space and outreach (Sharp et al., 2025; Kuhail et al., 2025; Garcia et al., 2020). In 2023, during a workshop organized by ESA/ESTEC (Figure 1.1), many XR applications were presented, highlighting the importance of further

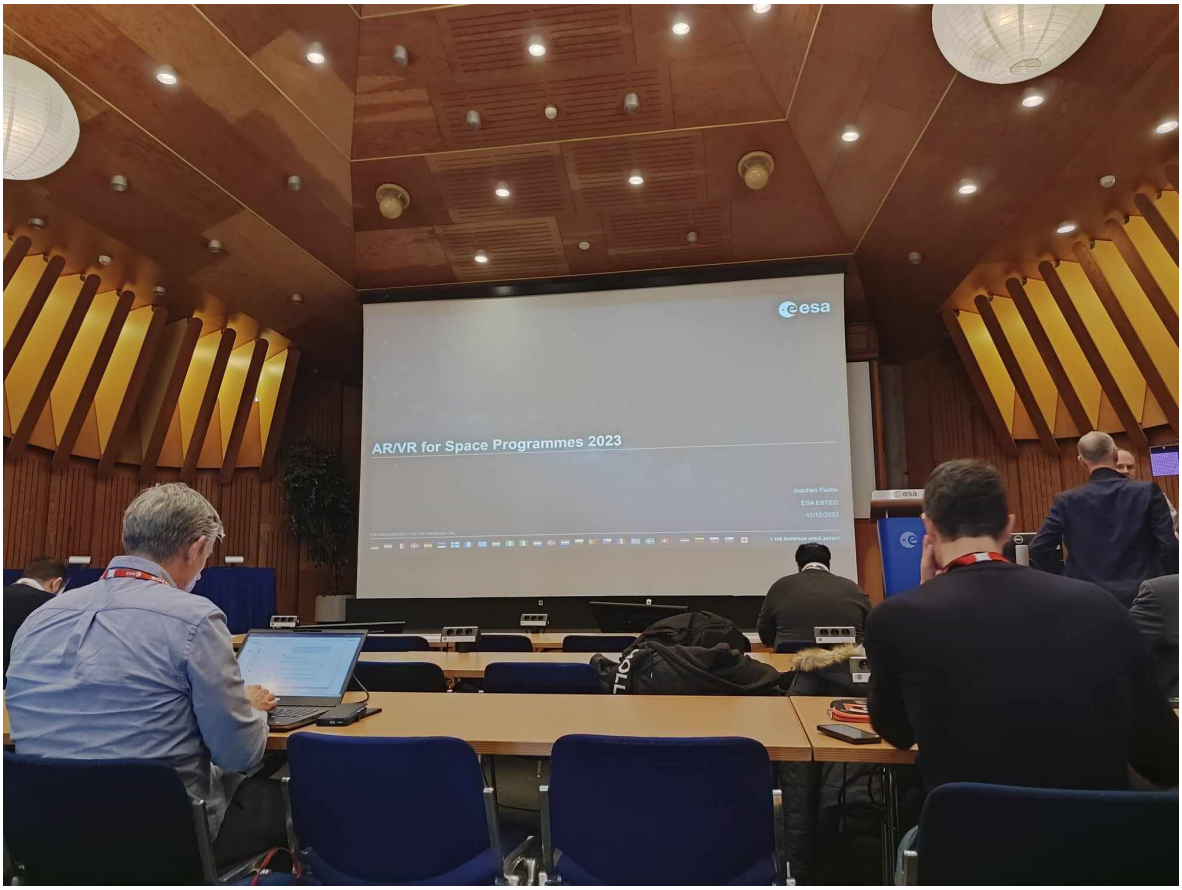

Figure 1.1: *AR/VR for Space Programs workshop (2023) at ESA/ESTEC. XR projects were presented, varying from remote operation, outreach, simulations, data visualization and astronaut training applications*

investigation of emerging technologies for the future of space exploration. In addition, although visualization has been extensively used in astronomy and space exploration, many previous works also highlight the fact that interactive and comparative visualization are underdeveloped, especially in 3D and need further research (Punzo et al., 2015; Lan et al., 2021). Particularly in planetary mapping, the majority of existing representations are either focusing on 2D or lack interactivity. For instance, one of the most characteristic examples is NASA's MoonTrek. MoonTrek is an online visualization website for science communication that allows users to navigate through our solar system and the moon, combining

both topographic and spectroscopic datasets.

From the existing research and applications the three following problems arise:

1. Maps are mostly 2D and lack interactivity.
2. Interactive 3D Visualizations focus on topography and not spectroscopy.
3. Most of the interactive 3D visualization in planetary mapping is used for public outreach rather than a scientific tool for.

1.3 Research Question and Goal

From the existing research, the following question arises:

"Can interactive 3D visualization enhance analysis compared to 2D maps in spectroscopy?"

To answer this question, we will develop a 3D visualization applying Human-Computer Interaction (HCI) principles and investigate how interactivity could help improve our understanding of complex datasets. Through this project, not only will topographic datasets be used, but the main focus will be on the 3D visualization and comparison between spectroscopic observations derived from Chandrayaan-1 Moon Mineralogy Mapper (M^3) and JAXA's MI Kaguya (SELENE). The purpose is to develop a high-fidelity prototype based on the above spectroscopic datasets that serves as an interactive research tool for astronomers. The final 3D product will be compared with a 2D version for evaluation.

The following sections introduce the project's case study and outline the importance of mineralogy in planetary science and specifically the relationship between minerals and elements, such as olivine and FeO. Moreover, the related research around interactive data visualization in planetary science will be explored as well as the use of Machine Learning for lunar exploration, in order to provide a clear picture of the use of data visualization in the field of planetary science.

To continue, in the section "Datasets" the necessary datasets for this project are introduced and the reasons why they were chosen, to continue with the "Methodology" chapter, where the full processing pipeline is described in details.

After the description of the project's steps that led to the development of the prototype version of the interactive 3D crater, the "Results" are presented. In this chapter, the interaction is discussed first with the evaluation outcomes of the testing to follow.

In the last chapter, the findings are described, leading to the answer of the Research Question. Afterwards, the "Limitations and the Future Improvements" are highlighted, where the limitations that were faced during the different stages of the development and evaluation of this project are being discussed. Thus,future implementations are being suggested to improve or expand the current project.

1.4 Case Study: Aristarchus Crater

To eliminate the computational effort and to make the project less time consuming, the idea of generating a global lunar map had been rejected. Thus, we have chosen to focus on one region of the Moon, and, specifically, the Aristarchus crater. Aristarchus is an impact crater, located on the near side of the Moon. It has a diameter of approximately 40 km with a 2,7 km depth from rim to floor. It is also one of the brightest and easily recognized spots on the lunar surface, even with a small amateur telescope. It owns its brightness to the high aldebo (reflectivity), and this is because, in lunar terms, Aristarchus is considered to be a relatively young crater with age of around 180 million years (König et al., 1977; Lucey et al., 2000; Grier et al., 2001; Zanetti et al., 2011a,b). Hence, its materials have not been darkened yet by space weathering as has happened with older craters (Gold, 1955; McKay et al., 1991; Hapke, 2001).

1.5 Olivine and FeO relationship

Regarding mineralogy, Aristarchus is a well-studied crater with evidence of the presence of olivine (Lucey et al., 1986; Le Mouélic et al., 2000; Yamamoto et al., 2010; Isaacson et al., 2011), mostly concentrated on the southeastern rim and the exterior of the crater (Mustard et al., 2011). Not only this, but also, Yamamoto et al. (2010) based on spectroscopic observations from Kaguya MI reported that olivine-rich areas are found in younger craters. In addition, Liu et al. (2011) using classification methods on multispectral data from Clementine analyzed the mineral composition of the lunar surface. In their study, one of the minerals examined was olivine, and specifically the correlation of FeO (ferrous oxide) and MgO (magnesium oxide) with olivine. Compared to pyroxene and plagioclase, olivine exhibits higher values of FeO and MgO contents. This observation helps to distinguish olivine from pyroxene, which has lower FeO and MgO contents, and together olivine and pyroxene also have higher concentrations of FeO and MgO compared to plagioclase. This is explained by the fact that pyroxene and olivine are both mafic-rich minerals. At the same time, a region with higher FeO and Mg but lower Al (aluminum) and Ca (calcium) content is potentially an area with olivine existence (Zongyu et al., 2012). This shows that FeO is a bulk composition, meaning that precise mafic-rich minerals like olivine cannot be detected by considering FeO alone. It is a combination of different minerals that indicates this. Spectroscopically, olivine has a broad 1μm absorption band Figure 1.2, while pyroxene exhibits in both 1 μm and 2 μm bands. Thus, to separate olivine from pyroxene we should look at the percentages of FeO and Mg of the Region of Interest (ROI) along with the percentages of other minerals. This leads to the conclusion that mineral distribution and identification are complex processes that requires spectroscopic observations and analysis of multiple contents, like FeO/MgO and Ca/Al.

Since the concept of this project is the visualization of the spectroscopic data, it would be interesting to develop multiple maps for comparison, however, for

simplicity we focus only on FeO and olivine in the prototype. Data will be further explained later in the section “Datasets”.

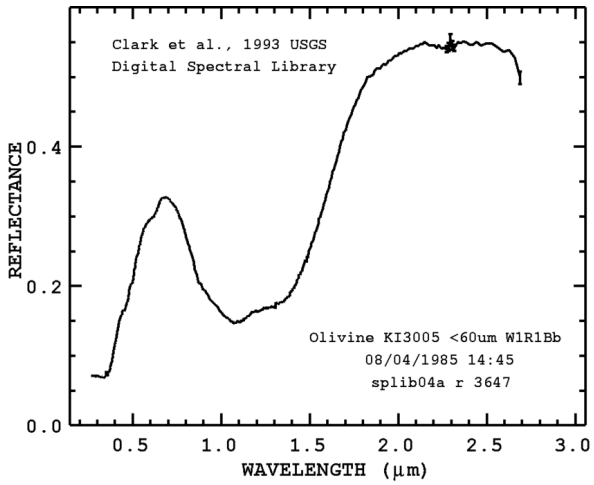

Figure 1.2: *The reflectance spectrum and the absorption band of olivine, as it is observed near 1μm. Data from USGS Digital Spectral Library (Clark et al., 1993)*

2. Related Work

2.1 Human-Computer Interaction and Data Visualization in Planetary Science

2D datasets for planetary mapping already exist in the literature. A typical example of 2D analysis and comparison of a lunar crater based on two different instruments and missions can be seen in Surkov et al. (2025). This study investigates ways to improve the resolution of mineralogy maps combining the datasets from M^3 (offers high spectral and low spatial resolution) and Kaguya MI (offers high spatial but low spectral resolution). Although the scope of this study was to improve the resolution rather than the visualization and the comparison between the datasets, it is a clear example of the 2D maps available today that lack interactivity.

However, as discussed previously, building a 3D interactive map of the lunar surface is not novel. Similar works already exist, such as Dong et al. (2013), but were mostly developed for outreach while focusing on the topology of the lunar surface excluded features like the per pixel analysis for mineralogical exploration. Other studies refer to 3D visualization based on Digital Elevation Models (DEM) with combination of spectroscopic observations (Barker et al., 2016; Thesniya et al., 2020), however they lack on interactivity. Their approach is limited to visualization rather than developing a 3D interactive map.

Furthermore, projects like DUST (Digital Lunar Exploration Sites Unreal Simulation Tool), a graphical environment for desktop application, was developed by Bingham et al. (2023) to support the Artemis program. The project focuses on surface level features on the contrary with similar applications and tools, like NASA's Moon Trek, which is entirely for visualization and not a tool for analysis. DUST is mostly developed for operational conditions, terrain and lighting, without focusing on mineralogy and spectral data. Another interactive desktop application is 3DView, developed by Génot et al. (2018). Although it is an interactive 3D visualization tool, it mainly focuses on 3D generated scenes for spacecraft trajectories and plasma.

At the same time, VaMEx-VTB, a VR project for planetary exploration and mission planning has been developed by Weller et al. (2021), however, it focused on topography and mission logistics rather than spectroscopic observation. A project that combines planetary exploration and spectroscopy in VR is VISor (Gold et al., 2021), which is based on in-situ and remote sensing data. Through

this emerging environment the users can walk around the 3D visualization of the surface (lunar or Martian) and from any point/pixel they can retrieve its reflectance spectrum. Thus, unlike other applications, it is an interactive tool based on spectroscopy, but not on Machine Learning analysis and does not explore nor compare extensively the mineralogical relations, an aspect that this thesis aims to investigate.

2.2 Machine Learning in Lunar Exploration

In recent years, Machine Learning (ML) has been a powerful tool used in Astronomy to extract information of existing datasets. As the datasets are rapidly growing and becoming more complex, the need for faster and more accurate data processing and analysis is also increasing. In astronomical research, two types of ML are mostly being used, Supervised and Unsupervised Learning. In Supervised Learning the model is trained based on an input dataset (ground truth), while in Unsupervised Learning the outcome is unpredicted and it is not based on any pattern or structure(Baron, 2019; Fotopoulou, 2024).

In supervised learning one of the most used algorithms is the Support Vector Machine (SVM) developed in 1995 by Vapnik et al. (1996) and it can be applied for both classification and regression problems. In this current study, one of the maps that has been used is the result of Support Vector Regression (SVR), which is a type of SVM and can be applied in fields such as lunar exploration and mineralogy.

In mineralogy and hyperspectral imaging, ML is used to study the lunar geology (Kodikara and McHenry, 2020), to compare and define similarities between earth and lunar basaltic rocks such as olivine and pyroxine (Fazel Hesar et al., 2025) as well as to extract mineralogical maps of specific elements in order to study the evolution of planetary surfaces like the moon (Bhatt et al., 2012, 2015; Bhatt, M. et al., 2019). Elemental and mineralogical maps of the lunar surface, in our case FeO abundance maps, are helping to study the evolution of the basaltic volcanism on the Moon, using multiple spectroscopical datasets.

Apart from mineralogy and lunar geology, ML is also important for future lunar missions, such as the Artemis program, planning to investigate the lunar surface and topography. From that perspective, ML can support future landing sights and classify minerals on the lunar surface using in orbit instruments (Liu et al., 2025; Peña-Asensio et al., 2025).

3. Datasets

3.1 Topography

Because of the numerous space missions related to lunar exploration, a huge amount of data already exists and are accessible online on NASA and ESA platforms. One of these platforms is `trek.nasa.gov`, from which the first datasets were downloaded for the purpose of this project.

More specifically, for visualizing the Aristarchus crater and any lunar area, topographic data are required. Through this website, a Digital Elevation Model (DEM) using data from Lunar Orbiter Laser Altimeter (LOLA), an instrument onboard Lunar Reconnaissance Orbiter (LRO), can be generated. Hence, the 3D topographic version of the Aristarchus crater was generated and downloaded as a 3D OBJ file from this platform (Figure 3.1).

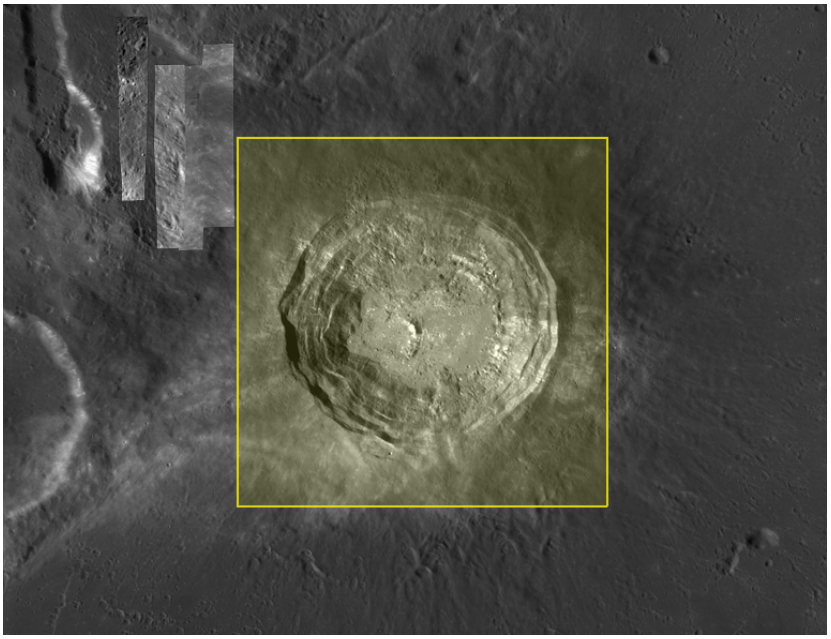

Figure 3.1: *The window of the Aristarchus crater, as it was cropped from trek.nasa.gov.*

3.2 Spectroscopy

Despite the topographic data, spectroscopic ones were also important for the visualization. The JAXA/SELENE/Kaguya MI mission was selected, and more specifically a mosaic from the topographically corrected Multiband Imager reflectance data of the Moon (Ohtake et al., 2013). These corrected reflectance data were processed to a global mosaic by Lemelin et al. (2016), which presents the abundance of olivine on the lunar surface expressed as weight percent (wt%). In the colorized mosaic (Figure 3.2), and thus in our Region of Interest (RoI), higher abundance of olivine is presented in green color, while lower abundance of the mineral is depicted in blue. Also, the MI instrument is a high-resolution multiband imaging camera that consists of five sensors in visible bands (415, 750, 900, 950, and 1000 nm) and four in near-infrared bands (1000, 1050, 1250, and 1550 nm) (Figure 3.3). In our case, the chosen mosaic was resampled to 512 ppd (which corresponds to 59 meters/ pixel) from the original resolution of 2048 ppd (15 meters/pixel). From this mosaic, the same region as the DEM was selected and the file was downloaded in PNG file format to be used as texture layer for comparison.

All of the datasets from the space missions can be also found on Planetary Data System (PDS), however in raw format and in need for pre-processing before they can be used for visualization.

For the comparison, a second global mosaic was used. The mosaic was based on datasets from Moon Mineralogy Mapper (M^3), a hyperspectral imager on Chandrayaan-1 (CH-1) spacecraft (Figure 3.4). The final map was generated using Support Vector Regression (SVR) by Bhatt, M. et al. (2019). In order to train and validate the SVR model for FeO abundances on the Moon, the authors used as reference data from the Kaguya Gama-Ray Spectrometer (KGRS). The final global SVR_FeO map (Figure 3.5) was in GeoTiFF file format with a resolution of 20 ppd (pixel per degrees). This map was used as the second texture for the visualization and the comparison with the olivine map. The exact stages of processing are described in the following section.

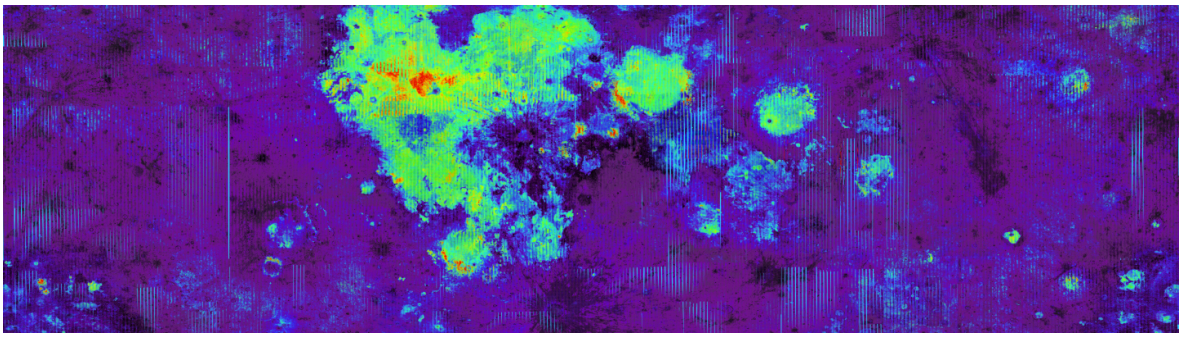

Figure 3.2: *Global map of Olivine. Data produced by JAXA/SELENE Kaguya MI (Ohtake et al., 2013)and processed from Lemelin et al. (2016). Blue shows low concentration of olivine and green higher.*

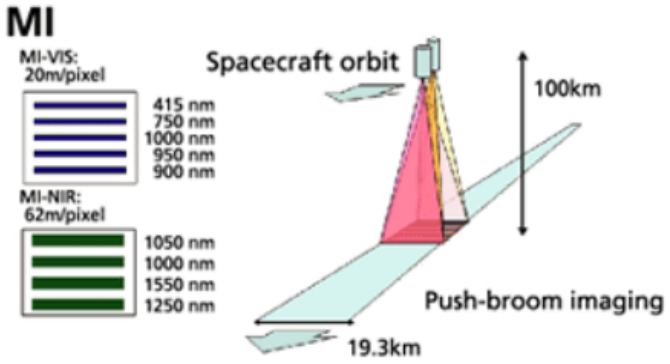

Figure 3.3: *KAGUYA Multiband Imager (SELENE mission) illustration, credit: JAXA.*

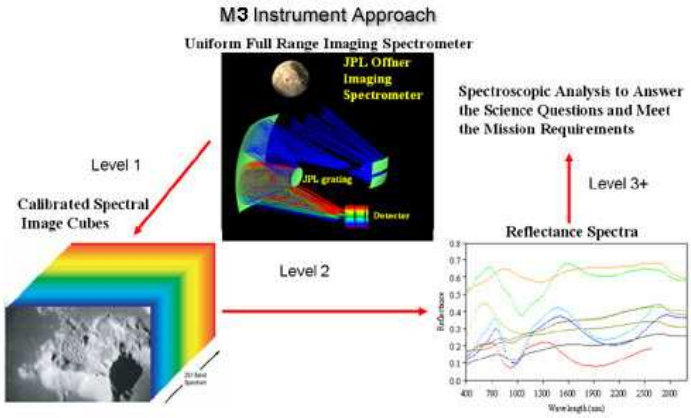

Figure 3.4: *Chandrayaan-1 M3 instrument and reflectance spectra, credit: NASA / JPL / ISRO / M3 team.*

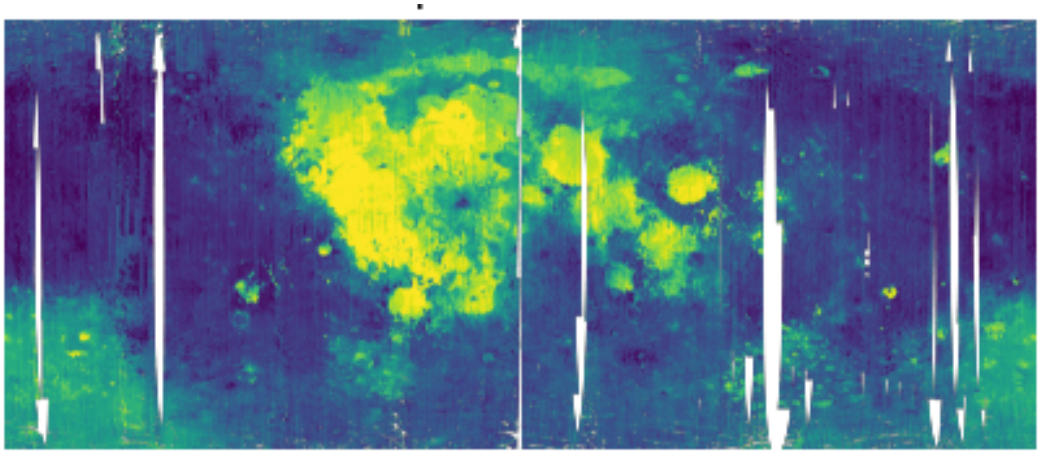

Figure 3.5: *Global map of FeO, as it was generated using ML SVR by Bhatt, M. et al. (2019). Blue color represents low FeO abundances, while yellow is used medium to higher values.*

4. Methodology

4.1 Pre-Processing

The processing can be divided in two stages: the Pre-Processing and the Main Processing - Visualization stage. After data collection it was important to crop the exact area of Aristarchus crater at the SVR_FeO map, matching the same Field of View (FoV) of the Kaguya's area. In the pre-processing stage python was used to calculate the window, crop the area and generate a similar LUT to the one as used in Bhatt, M. et al. (2019).

First, the exact geographic bounds of the SVR_FeO map were known because of the metadata that a GeoTiFF file format holds. Additionally, the exact coordinates for the Kaguya texture and the 3D terrain were also known and provided when downloading through NASA Trek website (-48.4150 to -46.5188 (lon), 22.7728 to 24.6625 (lat)). Knowing that, the geographic coordinates were converted to pixel indices in the SVR_Feo GeotiFF using rasterio.index(). Thus, the cropped region of the Aristarchus FeO map was cropped to match the exact same spatial extent of the Kaguya's olivine map and the LRO DEM terrain (53 x 57 km). The coverage in kilometers was important to be calculated:

$$-46.5188 - (-48.4150) = 1.8962^\circ \quad \text{for Longitude Range}$$

$$24.6625 - 22.7728 = 1.8897^\circ \quad \text{for Latitude Range}$$

We also know that on the Moon:

$$1^\circ \text{ latitude} \approx 30.3\,\text{km}$$

$$1^\circ \text{ longitude at } \sim 23^\circ N \approx 27.9\,\text{km } (\cos(\text{latitude}) \times \text{lunar radius scaling})$$

Thus, the coverage in approximation is:

$$\text{East–West} \approx 1.8962 \times 27.9 \approx 52.9\,\text{km}$$

$$\text{North–South} \approx 1.8897 \times 30.3 \approx 57.2\,\text{km}$$

After cropping the RoI, a colormap Look-Up Table (LUT) was applied on the FeO texture. The Jet version was selected for the generated LUT with fixed normalization, in order to match the global FeO w% scale in Bhatt et al. (2019). The image was resized to 400 x 400 pixels, matching the Kaguya's resolution and then saved as a PNG file.

4.2 3D Visualization

For the main processing and development of the interactive visualization, Godot v4.3 was used, which is an open-source game engine, suitable for 3D and VR development environment. For the 3D terrain representation the LRO LOLA elevation model was used. On top of the terrain, the two textures (Kaguya's olivine map and Bhatt's FeO map) were added. To the interface, a slider was added to control the transparency of the overlapping texture, revealing the bottom texture for comparison. In the main scene, apart from the 3D object, additional aspects were also taken into account, such as the direction of light, and the camera settings, providing a more realistic final result. Furthermore, two side bars were also added to the interface, giving a visual explanation of the mineralogical distribution of the textures (Figure 4.3). In Figure 4.2 a general workflow diagram is presented and in Figure 4.1 a visualization of the used datasets.

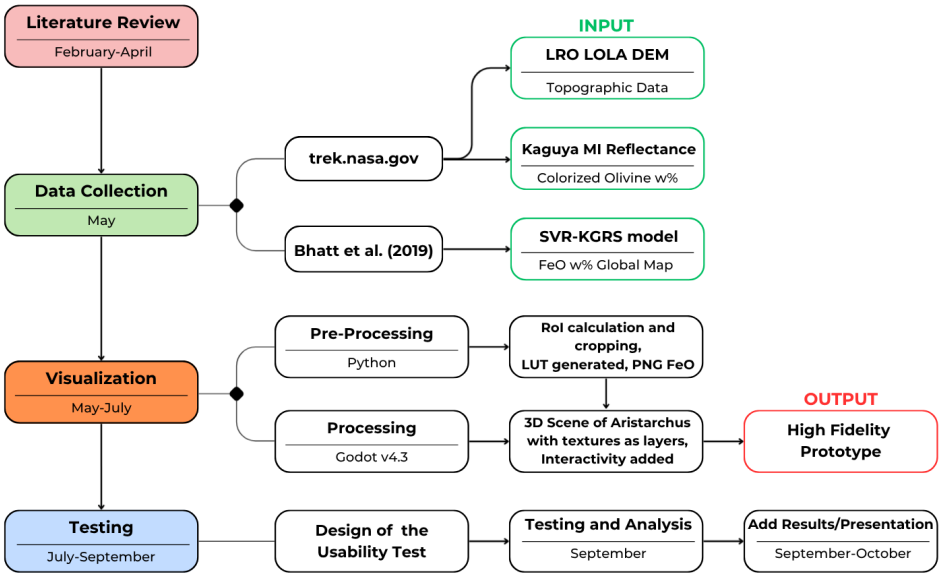

Figure 4.1: Representation of the project's workflow.

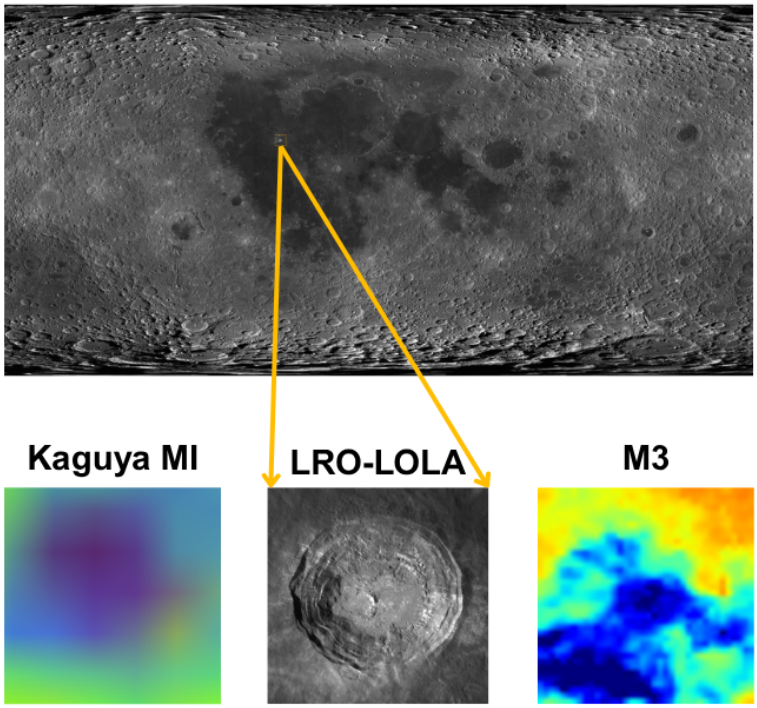

Figure 4.2: The 3 different inputs used for the visualization. In the middle, the cropped version of the crater and the topographic data from LRO-LOLA, dowloaded as 3D OBJ to serve as mesh terrain. On the left, cropped version from Kaguya MI and olivine representation, used as the first texture on top of the mesh terrain. On the right side cropped version of FeO, data from M^3 processed by Bhatt, M. et al. (2019), and used as the second layer-texture.

4.2.1 FeO w% Calculations

What makes this project an analysis tool for mineralogy rather than a basic 3D visualization is the addition of per-pixel analysis across the Aristarchus region. The idea behind this feature was to create an interactive visualization making use of Machine Learning output. The FeO global map is the result of SVR and depicts the abundances (w%) of iron oxide with false colors. Visually, the LUT map is very useful for providing an overview of the mineralogical distribution. However, the map by itself cannot provide precise information, especially for every pixel separately. To do so, further processing was needed.

Luckily, the initial global map was in GeoTiFF file format, meaning that allows georeferencing and retains hyperspectral information. Thus, the result for every pixel was preserved and it was easy to be retrieved and used at the visualization. Once again the exact same region around the Aristarchus crater was cropped using the given coordinates and following the same technique as above with the terrain's geographic footprint and rescaled to 400 x 400 to match the terrain's

resolution. The cropped image was exported as an RGBA PNG file format, where RGB = Red, Green, Blue, and Alpha = Opacity, to avoid blending or transparency issues during import to Godot. RGBA means that every pixel has Red, Green, Blue and Alpha channels, with integer values ranking from 0 to 255. On the other hand, FeO values are decimals (e.g. 10.57 w%) and because RGB channels store integers, each FeO decimal was multiplied by 100 (e.g. 10.57 x 100 = 1057). However, the resulted integers exceeded 255, thus every integer was split into two channels, Red and Green, with Blue = 0 and Alpha = 255 (100% opacity). To retrieve the FeO w% value back we combine Red and Green channels and divide the result by 100. This can be expressed by the formula:

$$\text{FeO } w\% = \frac{R \times 256 + G}{100}$$

where R is the most significant byte.

Afterwards, this image was imported to Godot and used as a hidden data map. To link the coordinates of the 3D mesh with the 2D image we first have to define the coordinates (UVs) of the hit-point P. By clicking on a point at the 3D mesh we hit a spot inside a triangle (ABC), because 3D objects are made of small triangles. The exact UV coordinates of the triangle can be calculated as:

$$P = u \times A + v \times B + w \times C$$

where u, v, and w are the weights. These are called barycentric coordinates (u, v, w).

Thus, barycentric coordinates describe how close to each corner is the hit point. To calculate the coordinates of that specific point and knowing the barycentric coordinates of the vertices, we compute barycentric interpolation. The formula of the UVs of the hit point P inside a triangle ABC is computed by the weighted average of the UVs at the triangle's vertices and it can be expressed as:

$$\text{UV}_P = u \times \text{UV}_A + v \times \text{UV}_B + w \times \text{UV}_C$$

Lastly, to match the UV coordinates with a pixel on the 2D hidden map we multiply the U with the image width and the V with the image height, which in our case is U x 400 and V x 400.

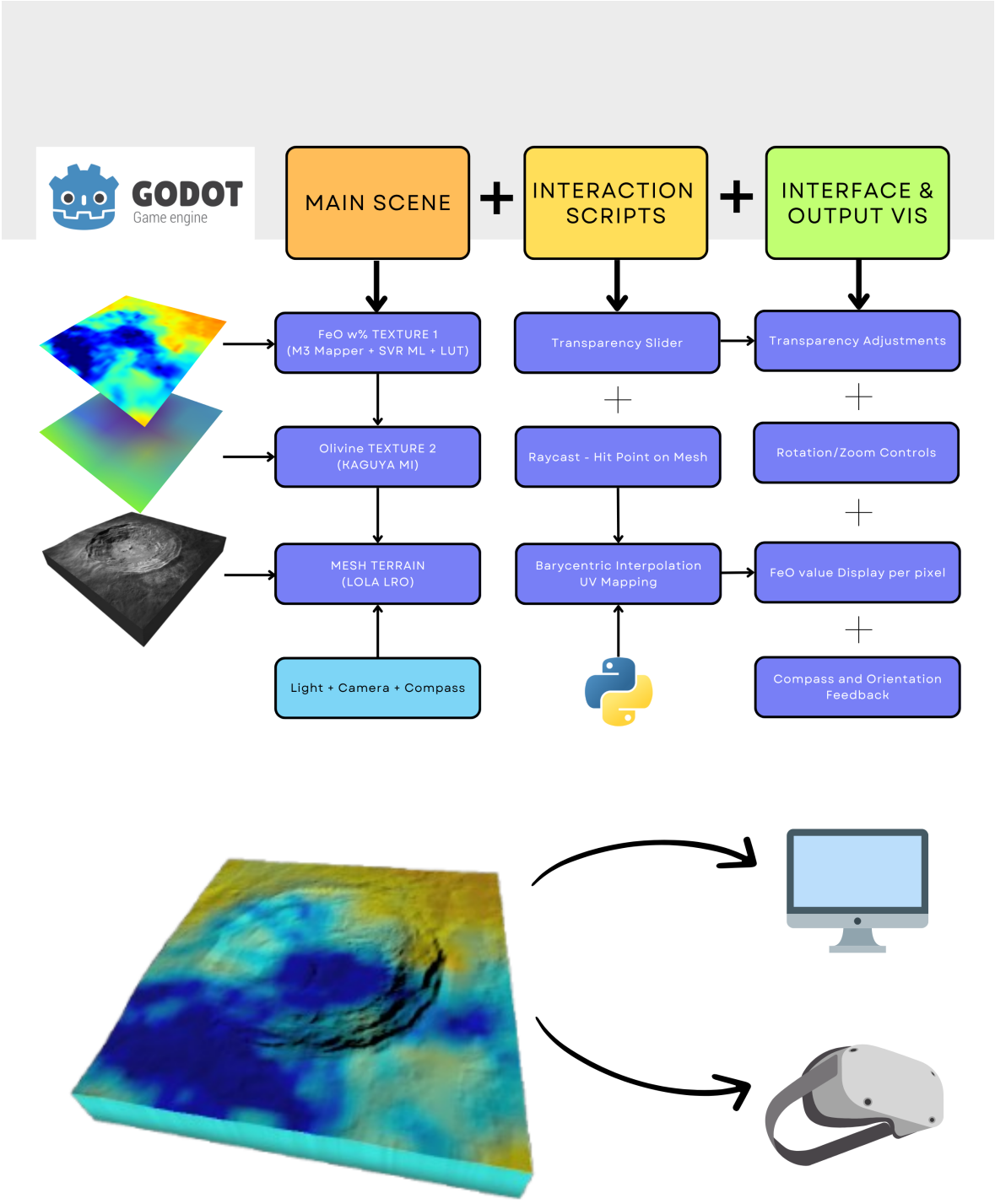

Figure 4.3: *Godot architecture pipeline. The prototype is designed for desktop and VR environments.*

4.3 Evaluation Design

An evaluation test was designed in order to assess the project. However, before outlining the test design it is crucial to point out the main goal of the evaluation, present the further steps required and defined the target group of participants.

The primary objective, which was also the research question, was whether an interactive 3D visualization can enhance analysis in spectroscopy compared to a static 2D map. Thus, the effectiveness of the 3D visualization needs to be examined and compared with the effectiveness of the same 2D version of the map. For this reason, prior processing was needed. As it was already described above, a region around the Aristarchus crater was cropped from the global FeO map, generating a LUT to represent the w% of iron oxide. To improve this 2D version and in order to add interactivity, the same RGBA PNG file previously used in the FeO hidden map on the 3D was applied. This image was then aligned with the texture and placed on top of that with an opacity set to 0, creating an invisible FeO heatmap. Consequently, when any pixel on the image was clicked, a box displayed the pixel's coordinates and the FeO w% for the exact same pixel. An example of the 2D version of the visualization can be seen in the Figure 4.4.

Another important aspect to take into account was the definition of the participants. At the beginning the target group was specifically consisting of astronomers and planetary scientists, however this was shifted to a broader audience including people from the STEM domains. This parameter changed to simplify the experiment and attract more participants.

After developing the interactive 2D version for the testing and defining the target group of the participants it was time to receive consultation from the experts. To be more exact, one expert came from the field of computer science, one from physics, and two from astronomy. In general, their opinions and suggestions regarding which areas to test and what is important to include in the evaluation were valuable as they shaped the final form of the test.

The testing was divided and developed in the following three parts:

Part 1. Task Performance (Quantitative Data)
Part 2. Questionnaire (Quantitative Data)
Part 3. Open Feedback (Qualitative Data)

Part 1

Tasks in Part 1 were design based on Shneiderman's Visual Information-Seeking Mantra (Shneiderman, 1996) and the mantra of designing the evaluation for information visualization. Based on Shneiderman (1996) overview comes first, then zoom and filter and lastly the details on demand. Users have first to

overview the visualization, to get a clear and general picture of it. Then, zooming in they focus on specific areas of interest, filtering unnecessary data. Lastly, users had to interact with a specific element of the visualization, to evaluate the details on demand.

Having Shneiderman's principals on mind, in the first part, three easy and short analysis tasks were assigned to the participants. The concept of task 1 was to give the users a short task for the 2D version, such as reporting the FeO values of 2 different spots on the rim. The second task was the same, but this time was on the 3D version. The idea behind that was to examine if the geological features were easily recognizable in a spectroscopy map resulting from ML and compare the 2D and 3D version respectively. In this way, accuracy and understanding were tested. Task 3 was focused on the effectiveness of the transparency slider on the interface and the comparison of the 2 overlapping maps (FeO and olivine). At this stage, a random region was chosen for visual comparison based on the LUTs, the sidebars and the transparency feature, in order to test data interpretation. For all the tasks in Part 1 the time to complete the exercises was recorded (for further task performance analysis) and the users had to answer whether or not the task was easy after the completion of every step.

Part 2

In this part users had to answer 6 questions in total and reply using a Likert scale, choosing between 1 and 5 (1 = strongly disagree, 5 = strongly agree). This stage was designed to evaluate usefulness and perceived usability. The purpose was to examine how easy and clear the tool was to use compared with the 2D version, the visual comparison using the slider and whether they were willing to use a similar tool again in research or teaching. In total, six questions/items formed part 2.

Part 3

In this last part the users had to provide feedback through two open questions. The first one was "What did you like the most about the 3D visualization" and the second one "What was confusing, difficult, or could be improved?". The aim of the questions was to ask for one positive (first) and one negative (second), which would provide feedback for future improvements.

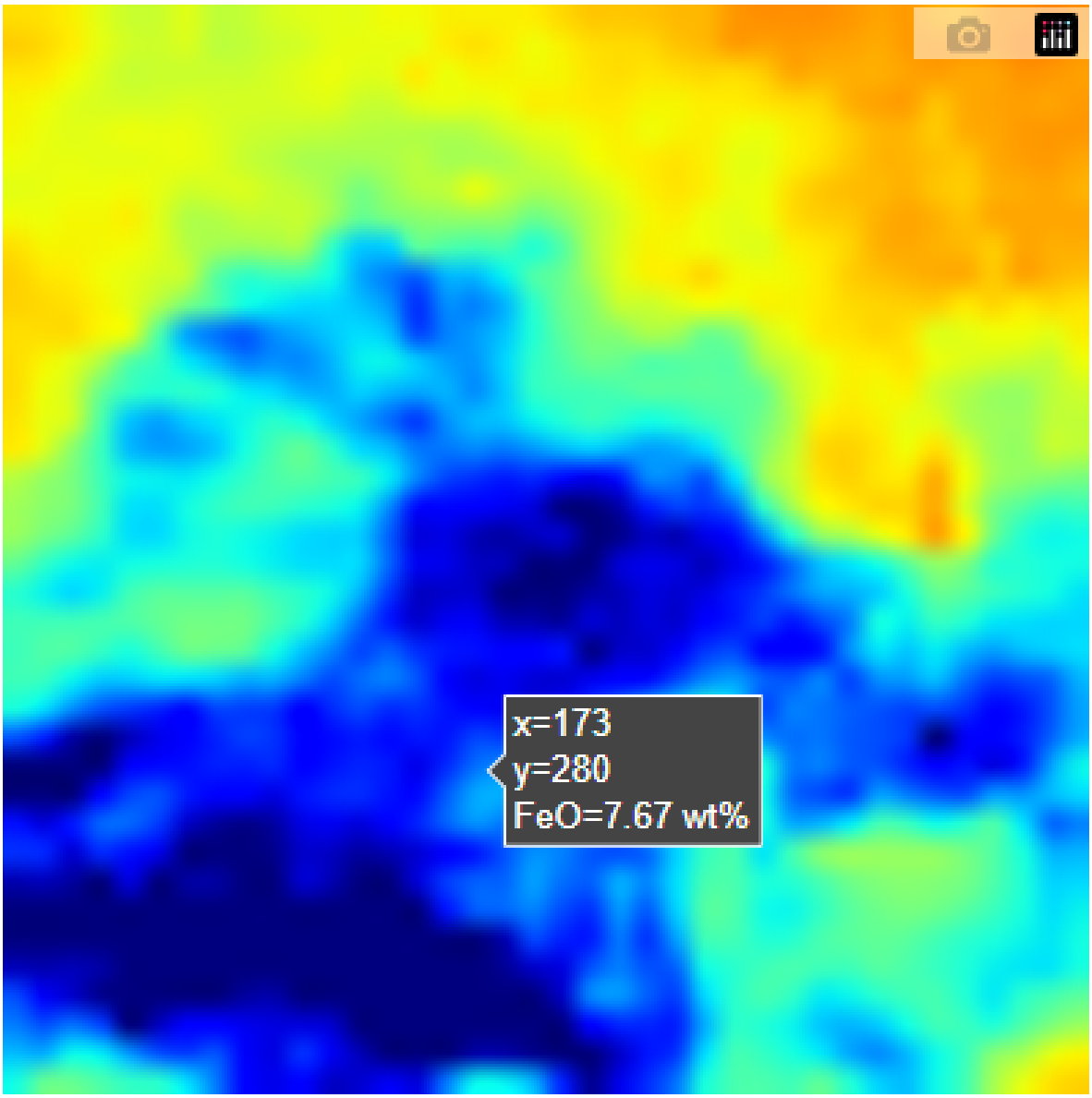

Figure 4.4: *The 2D map of FeO. Users place the mouse on the surface and receive the coordinates of the pixel and the FeO w%. The map was build for comparison with the 3D map. This 2D interactive version developed with Python in Google Colab.*

5. Results

5.1 The Prototype

The 3D Visualization of the Aristarchus crater is a high-fidelity prototype, meaning the project is close to the final product. The project can be downloaded from GitHub. It contains basic interactive heuristics, such as zoom in and out and rotation. It also contains a mouse slider that adjusts the transparency of the overlapping texture, allowing viewing both of the textures, as it was described above (Figure 5.2). Apart from the slider there are 2 LUT bars, providing feedback about the depicted false colors and the distribution of the minerals on each map. The role of the side bars is to reduce users' cognitive load. The distribution of the minerals is expressed in weight percentages (w%) for both of the maps and there are three labels (Low, Medium, and High) to help users observe the percentages with clarity (Figure 5.1).

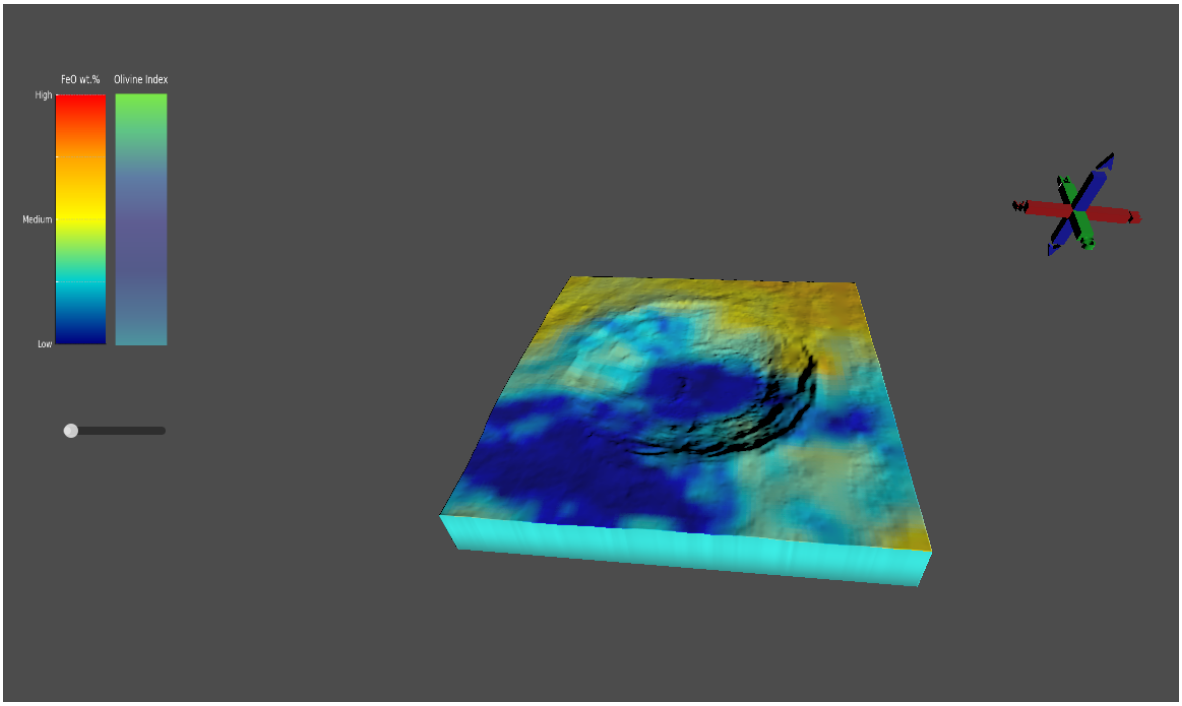

Figure 5.1: *The initial interface of the project in run mode. The FeO map is visible.*

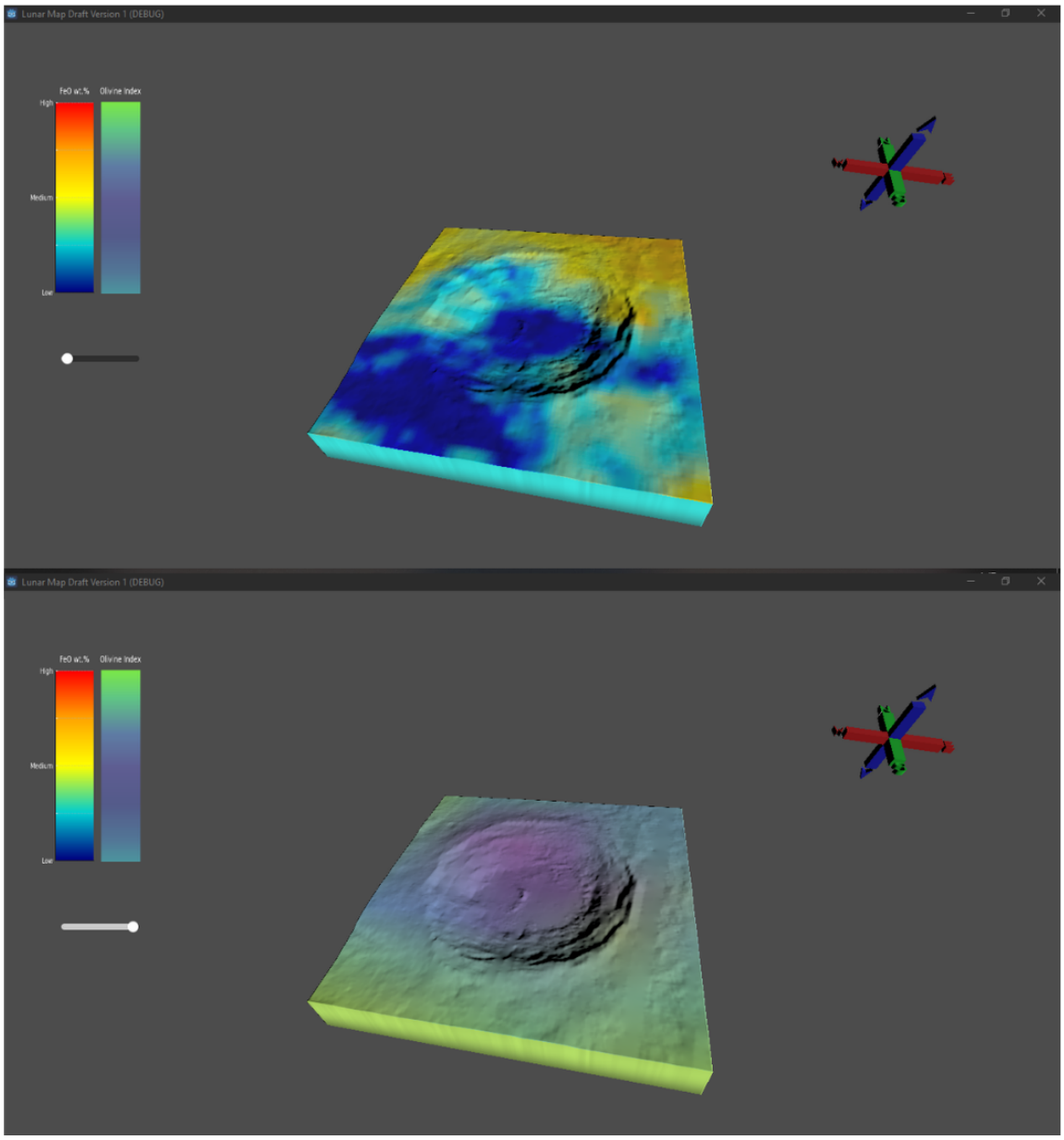

Figure 5.2: *The slider controls the transparency of the FeO map, allowing the view of the olivine map bellow.*

In addition, the User Interface (UI) was built in a way to help researchers compare complex mineralogical data with existing datasets in spatial context. Not only this, but the design of the interface also remained as simple as possible to avoid errors during the interaction and to maintain user's mental model. The interface is easy to handle and the users receive clear feedback while interacting with the object. Moreover, the addition of a compass in the final visualization enhanced the orientation feedback while rotating the crater.

Moreover, this project is built as a scientific tool for mineralogical maps based on spectroscopy. Despite the orientation features, what distinguishes this visualization is the addition of the per-pixel analysis. By selecting a pixel on the area, a generated result appears in the console, displaying the FeO w% and the coordinates of that specific pixel (Figure 5.3).

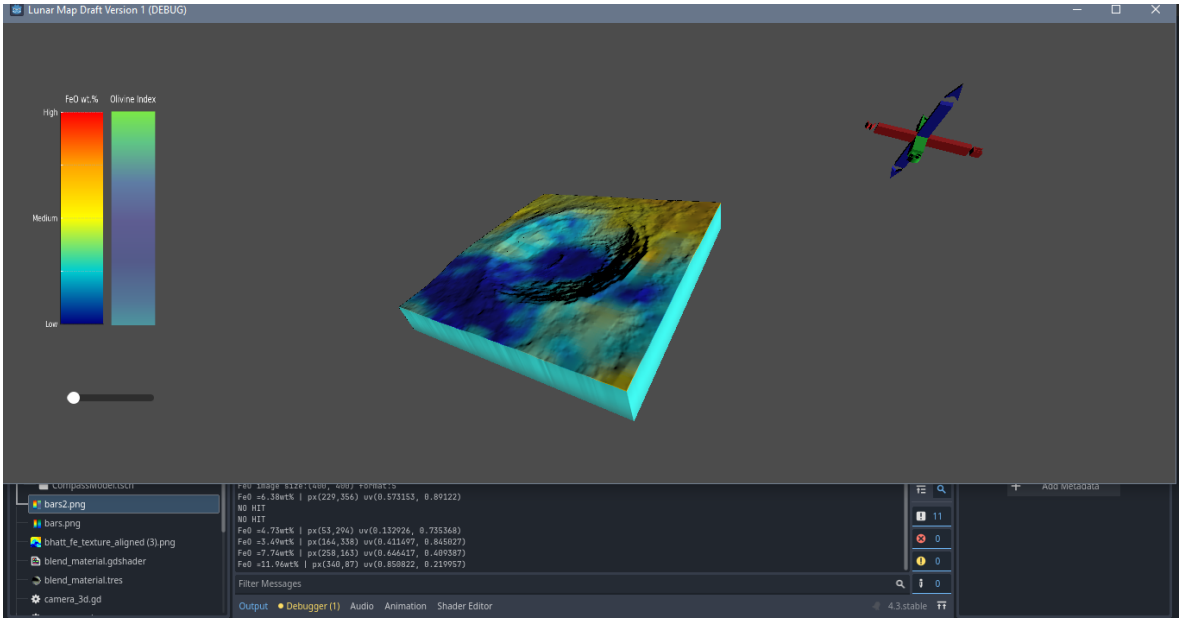

Figure 5.3: *The FeO w% and the pixel's coordinates are displayed at the game engine's console. If the mouse clicks outside of the crater, the console shows "NO HIT", giving feedback. If the mouse clicks the surface an FeO value appears. Transparency changes, rotation or zoom in and out do not affect this feature.*

5.2 Evaluation Test Results

The total number of participants was 15 ($n = 15$) and they were all coming from STEM fields. In general, participants completed all the tasks in Part 1 in a few minutes. However, as it is shown in Figure 5.4, it took them significantly more time to complete task 1 compared to task 2. Users reported that it was not easy for them to identify any geological feature on the 2D map and they felt unsure where the rim was. On the contrary, it was easy for them to spot the rim on the 3D version, making them mark the FeO values faster and gave positive feedback after the completion of the second task. Another noteworthy point is

the performance pattern of the users. It seems that participants who required more time to complete the tasks in the 2D version were slower in the 3D as well. This indicates a positive association between the task completion in 2D and 3D versions (see Figure 5.5).

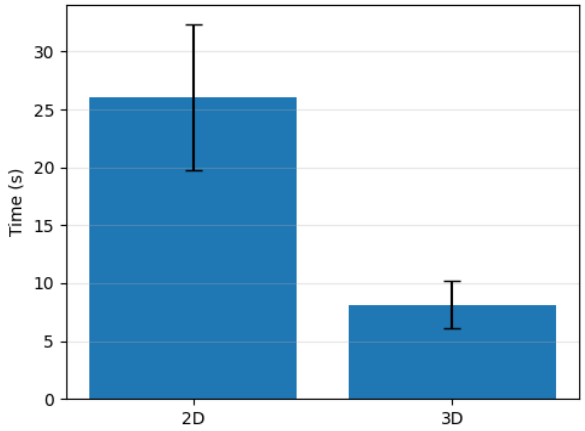

Figure 5.4: *Average time (in seconds) to complete Task 1 and Task 2 on the 2D and 3D maps.*

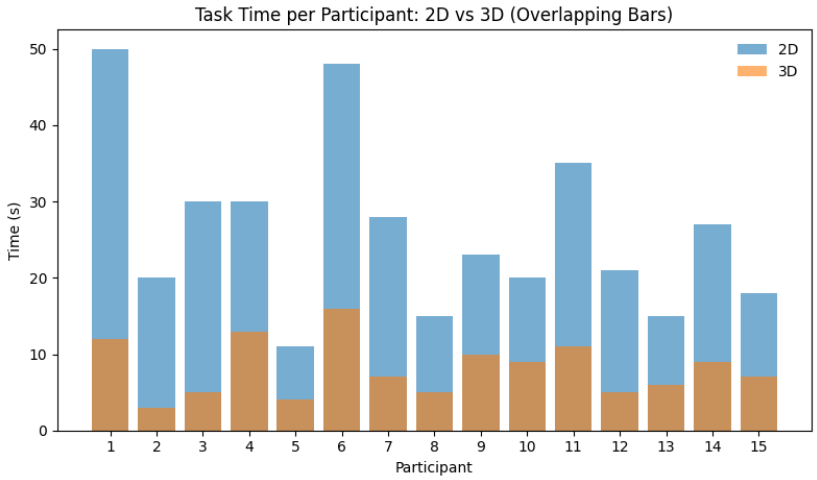

Figure 5.5: *Performance pattern of participants in the 2D and 3D versions, showing correlation in completion times.*

More specifically, Figure 5.6 shows that in the 2D version the users took an average of 26 seconds until they detect the rim, while the same task at the 3D version took an average of 7.6 seconds. We can also notice that in the 2D version some participants required significantly more time to complete the given tasks (45-50 sec). This leads to the result that the 3D tool reduced the time task, and increased the confidence in identifying geological features.

For the second part, the Likert items, participants had to evaluate the effectiveness and the usability providing responses on a scale from 1 (strongly disagree) to 5 (strongly agree) to the given questions/items. In Figure 5.7 the 6

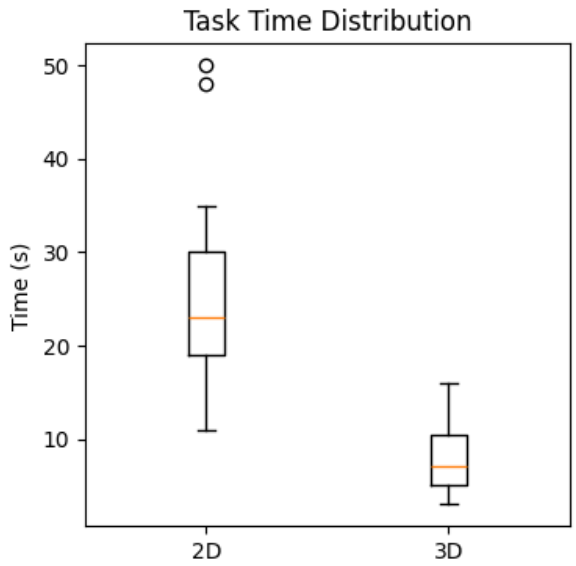

Figure 5.6: *In 2D participants needed in average 22 seconds. The majority of them scoring from 12 to 30 seconds,while 2 participants spent around 50 secons in the 2D. In the 3D the interaction time dropped in an average of 8 seconds, with most of them spending 5 to 12 seconds.*

items/questions are presented with mean scores with standard deviations as they are illustrated in Figure 5.8. In particular, the majority of the users agreed that the 3D was easy to use (answers varied between 4 and 5). In addition, almost everyone responded with 5 (strongly agree) regarding the clarity of the 3D map, while in the 2D version the scoring was lower, with the majority of the answers giving 1 or 2. Nearly all participants agreed that the 3D version, compared to the 2D map, enhanced their ability to interpret FeO values in a geological context. Moreover, most of them reported that they would consider using such a tool in their research or teaching (answers varied between 4 and 5).

Regarding the use of the slider a small decrease was observed (Figure 5.8). The answers varied between 3 and 5, resulting in a higher standard deviation error bar. Overall, the slider scored around 4 on average, meaning the slider, and thus the transparency feature, was effective and useful for visual comparison between the two maps, however, some find it uncertain or difficult to control.

In the open question, participants have been asked to provide feedback regarding what they liked and to suggest improvements if need be. In summary the feedback was positive, reporting that the interaction (zoom, rotation) improved their orientation, and that in the 3D visualization it was easier to distinguish the rim and report its FeO values. However, some suggested general improvements on the interface or the heuristics, such as the color intensity or the side bar improvement, because they needed more feedback during the tasks and the colors of the Kaguya texture were less intense compared to FeO texture (Figure 5.9) .

Item	Mean (SD)	Interpretation
The 3D tool was easy ti use	Mean = 4.67, SD = 0.49	strong agreement, high usability
Clarity of clicking in 2D map	Mean = 1.87, SD = 0.64	participants found 2D interaction unclear
Clarity on clicking the 3D map	Mean = 4.93, SD = 0.26	3D clarity rated very high
Slider aided comparison	Mean = 4.00, SD = 0.65	generally positive, some variation
3D improved geological interpretation	Mean = 4.93, SD = 0.26	near-unanimous agreement
Potential use in research/ teaching	Mean = 4.87, SD = 0.35	strong endorsement of future applicability

Figure 5.7: *Distribution of Likert scale responses for the 3D and 2D versions across six items.*

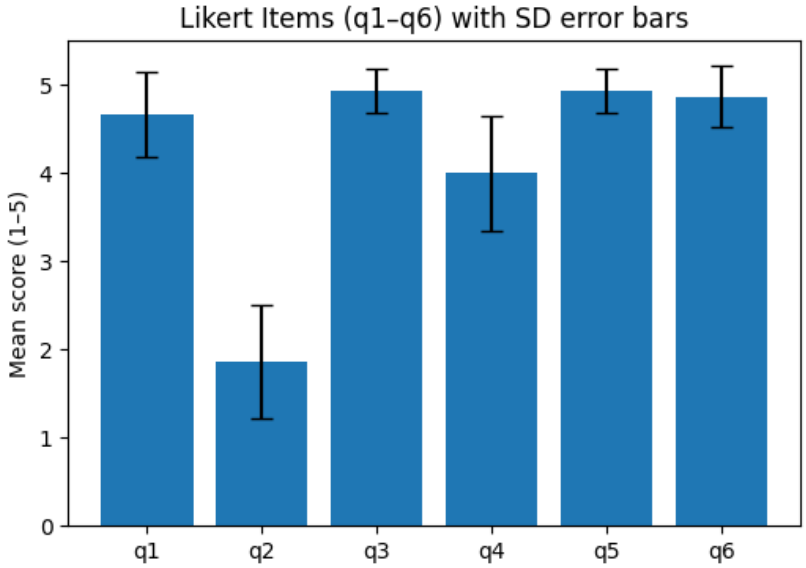

Figure 5.8: *The rating for the 6 items in Part 2 of testing.The spread of answers vary for each question. Q6 has one of the shortest spread of answers and scoring almost 5, meaning almost all of the participants are willing to use such a tool in their research and education.*

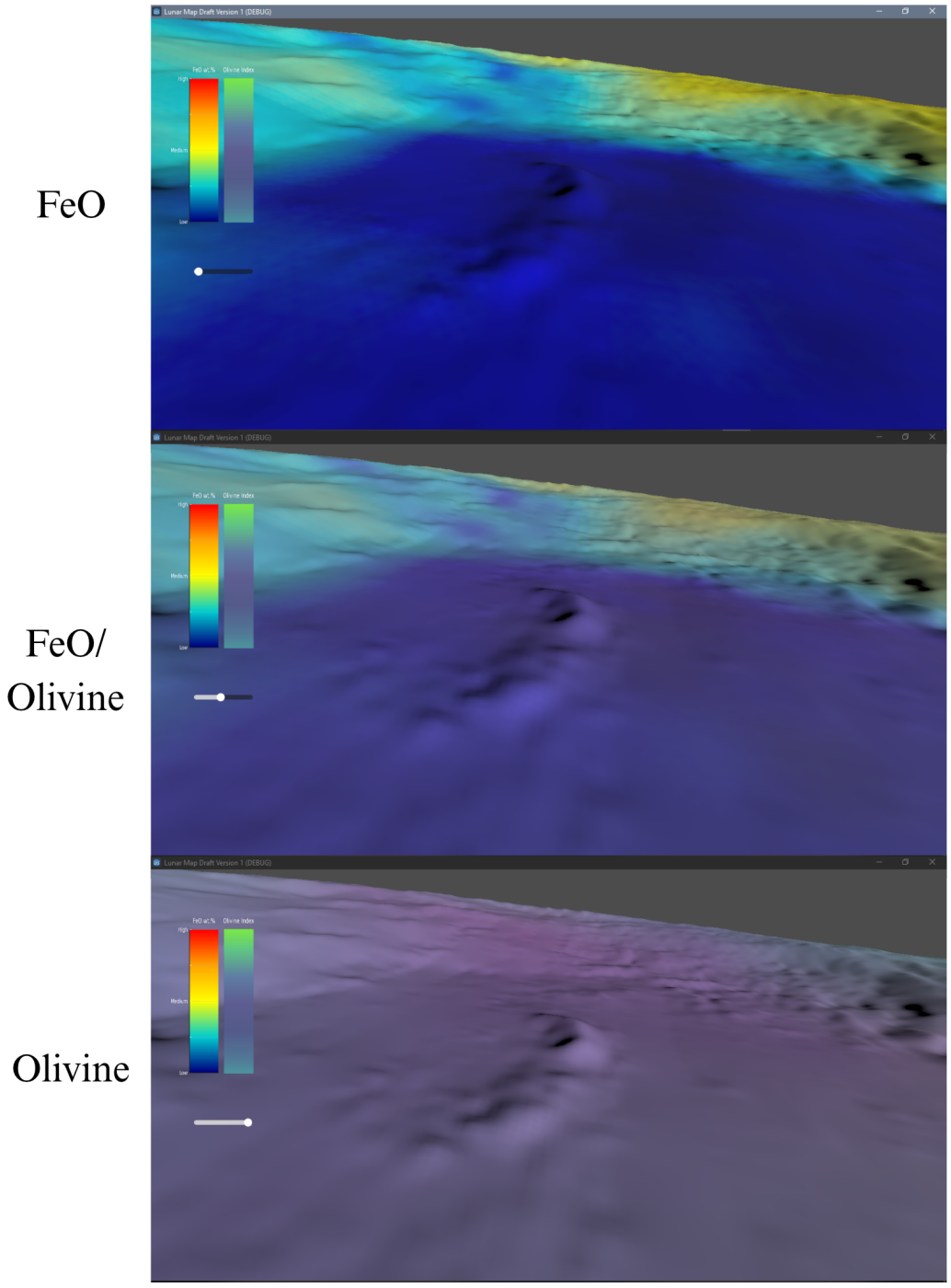

Figure 5.9: *Zoom in at crater's peak and transparency captured in stages. Transparency slider was in general scored high, but many participants suggested an increase on the olivine map for the future versions of the project. In this picture the transparency issue is depicted. From top to bottom: FeO map (without transparency adjustments), FeO and olivine blend (transparency at 50%), olivine(transparency 100%)*

6. Conclusion & Discussion

6.1 Conclusion

3D visualizations in science are not a novel approach. In the last few years, many studies have been conducted on the use of emerging technologies in space exploration and planetary science. Some of these applications draw attention to topography, while others were built as operation tools for space missions or outreach education. In any case, relevant studies in the field of planetary science suggest further research around 3D and VR environments focusing on interactivity and user engagement. However, fewer studies focus entirely on spectroscopy, especially using Machine Learning outputs for further analysis.

For this project, the Aristarchus crater was used as a case study for visualization. Aristarchus is one of the well-studied regions on the Moon with confirmed presence of olivine in the surrounding area. The 3D interactive visualization tool was developed for the comparison and analysis of the mineralogical distributions between two maps. Early results show that the prototype is promising, that participants were positive about using the 3D interactive tool at their research, while in general there is room for improvement and additional adjustments, including usability enhancements, more real-time feedback, and advanced spectroscopic analysis features. At the same time, users' performance improved significantly in the 3D version compared to the 2D. All of the above can increase the value of the visualization as a scientific tool for future research in the field of planetary science and exploration, while recent studies reveal its usefulness in other domains, such as Earth Observation.

6.2 Discussion

The aim of the study was to investigate whether the interactive 3D visualization can improve analysis compared to lunar mineralogical 2D maps. According to the results of the evaluation tests the 3D version is easier to handle, and less time consuming compared to the respective 2D map, making the 3D version more effective and accurate. Overall, the feedback was positive and participants reported that they would consider using a similar tool in their research, meaning a future further development of the project might be useful and promising. On the contrary, in the 2D map the participants had to reconstruct mentally the

topography in order to remember the geology and morphology of the crater and spot the rim. The results of this study also support previous findings on VR as a research tool. For example there are studies on interactive VR for analysis of volcanic topographic data concluded that 3D visualization can be a powerful tool researchers providing faster exploration (Zhao et al., 2019).

6.2.1 Limitations

One important limitation for the completion of this project was the processing of the datasets. Processing datacubes from hyperspectral imagers like the M^3 Mapper is a challenging task. The raw files need extensive processing to be ready for visualization and follow specific pipelines to reduce artifacts like the one that is used by Shkuratov et al. (2019). In general, there are not many 3D visualization that depict the results of ML. This was another reason why we have chosen to continue with the map from Bhatt, M. et al. (2019).

Another limitation was the fact that the whole lunar surface was not possible to be visualized. Such a task requires extensive resources and processing, as well as time, and that is the main reason why the final visualization was restricted to one crater.

Regarding the evaluation stage, one possible weakness is the total number of participants (n=15). One significant limitation was the number of people that could actually participate. This project is focusing on planetary science using spectroscopic observations, thus participants should not only come from a scientific background but also understand the topic. Having participants from irrelevant fields might influence negatively the results.

6.2.2 Future Improvements and Applications

To make this study more accurate and yield more confident results, further evaluation is needed in a larger audience and particularly focusing on a target group of planetary scientists and astronomers. Alternative methods to compare the 3D with the 2D version can also be applied, such as designing an A/B testing for side by side comparison and distinguishing the differences easier. Similarly, it might be interesting to test through A/B testing this version of the prototype and a second-future version with different interaction, and choose through testing which features are more convenient to keep.

From a technical perspective, many features can be improved, such as a smoother rotation or the intensity of the color maps, or the addition of the spatial coordinates with a scale bar for measurement. At the same time, there is also room for improvements regarding the User Interface (UI). To achieve this, more interactions can be included, which will lead to improve the current interface and integrate them. Lastly, as mentioned in the feedback, the intensity of the color of the maps can be enhanced and additional explanation or feedback regarding the sidebars might be helpful. In an improved version and for a future VR application, gamification elements could be added to increase engagement, especially if the visualization will be used for teaching.

Another future addition could be the coverage -if not the whole lunar surface at least the option- of multiple regions on the lunar surface using more minerals or different maps (Figure 6.1). Regarding mineralogy, and specifically olivine, lunar olivine can be a key mineral to enhance our understanding for other olivine-rich planetary surfaces such as asteroids (Sunshine and Pieters, 1998).

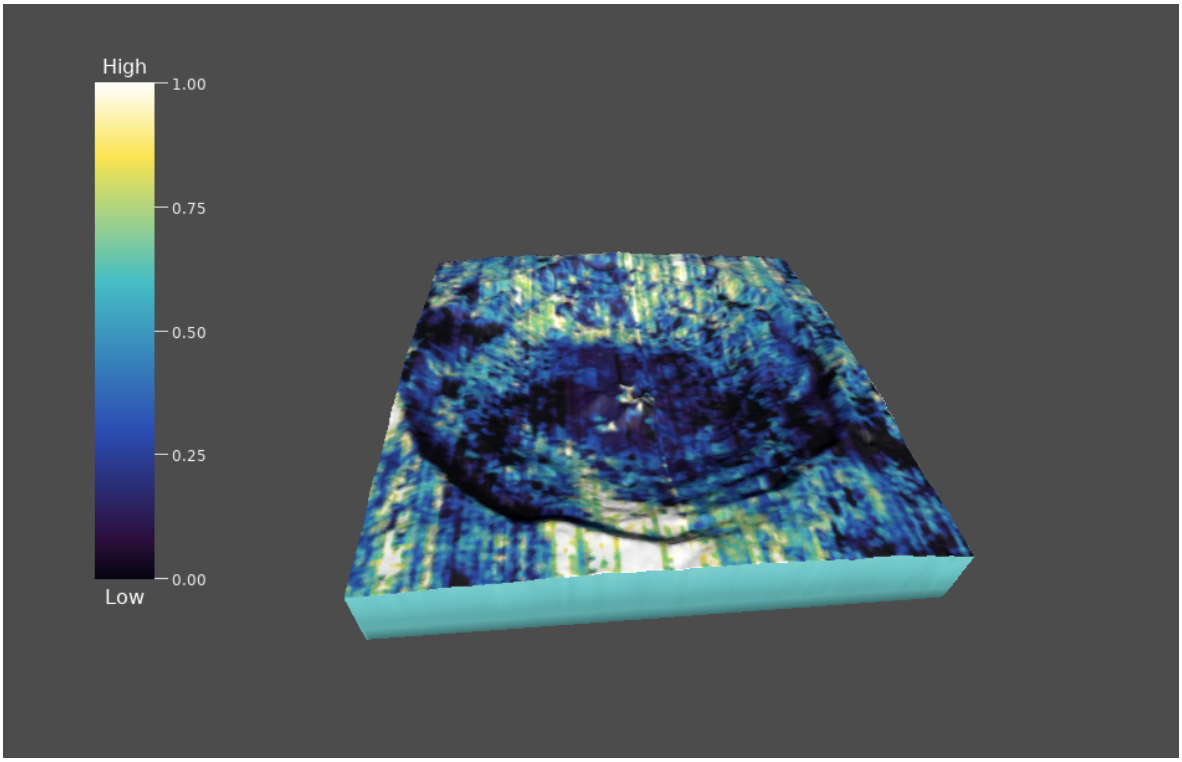

Figure 6.1: *Low fidelity prototype of the Bullialdus crater, as it was presented at International Astronautical Congress (IAC) 2025 in Sydney, Australia.*

Since olivine is expected in basaltic magmas, volcanoes on Earth are another place you can spot this mineral, thus there is already extensive research around olivine and volcanic rocks (Helz et al., 2017; Wallace et al., 2021; Su et al., 2022; Shishkina et al., 2023). Some relative studies are focusing on hyperspectral imaging on volcanic samples (Fazel Hesar et al., 2025). At the same time, over the last five years many studies are turning to 3D and particularly VR in geosciences, where VR has been extensively used. These studies highlight the need for further research in the future, particularly focusing on the interactivity (Ting and Wei, 2021; de Castro et al., 2026), while testing on similar approaches has shown that VR applications in the field could benefit researchers in their data analysis (Lin and Loftin, 1998; Lin et al., 1998).

From that perspective, it might be an interesting idea to develop a web-based platform for ML outputs that allows the creation of LUT for further comparison. Not only this, but also an interesting approach might be the applications of such interactive 3D visualization on asteroids or even Earth. Today, with the vast datasets from satellites and the high need for Earth Observation, an interactive visualization tool could be practical and beneficial for analyzing multiple and

complicated datasets (Gerloni et al., 2018). Similar works based on large satellite data have already started to be developed (Flatken et al., 2024), highlighting the potential and the strong demand for such applications.

Lastly, it should be noted that the current project is designed and developed in a way that allows deployment in VR environments. This approach could lead to additional implementations, tailored to the needs and the goals of the visualization. However, the per pixel analysis characteristic can be strengthened by integrated a spectroscopic graph generator for each specific pixel to improve the analytical capabilities of the visualization, and find new ways to improve user involvement, interaction and immersion in the VR environment.

References

Barker, M., Mazarico, E., Neumann, G., Zuber, M., Haruyama, J., and Smith, D. (2016). A new lunar digital elevation model from the lunar orbiter laser altimeter and selene terrain camera. *Icarus*, 273:346–355.

Baron, D. (2019). Machine learning in astronomy: A practical overview. *arXiv preprint arXiv:1904.07248*.

Bhatt, M., Mall, U., Bugiolacchi, R., McKenna-Lawlor, S., Banaszkiewicz, M., Nathues, A., and Ullaland, K. (2012). Lunar iron abundance determination using the 2-μm absorption band parameters. *Icarus*, 220(1):51–64.

Bhatt, M., Mall, U., Woehler, C., Grumpe, A., and Bugiolacchi, R. (2015). A comparative study of iron abundance estimation methods: Application to the western nearside of the moon. *Icarus*, 248:72–88.

Bhatt, M., Wöhler, C., Grumpe, A., Hasebe, N., and Naito, M. (2019). Global mapping of lunar refractory elements: multivariate regression vs. machine learning. *AA*, 627:A155.

Bingham, L., Kincaid, J., Weno, B., Davis, N., Paddock, E., and Foreman, C. (2023). Digital lunar exploration sites unreal simulation tool (dust). In *2023 IEEE Aerospace Conference*, pages 1–12. IEEE.

Brodbeck, D., Mazza, R., and Lalanne, D. (2009). Interactive visualization-a survey. In *Human Machine Interaction: Research Results of the MMI Program*, pages 27–46. Springer.

Clark, R. N., Swayze, G. A., Gallagher, A. J., King, T. V., and Calvin, W. M. (1993). The us geological survey, digital spectral library: version 1 (0.2 to 3.0 um). Technical report, Geological Survey (US).

de Castro, D. B., Ducart, D. F., de Sena, Í. S., de Lima Picanço, J., da Silva, C. H., and da Mota, G. S. (2026). Virtual reality in geoscience: An overview. In De Paolis, L. T., Arpaia, P., and Sacco, M., editors, *Extended Reality*, pages 20–38, Cham. Springer Nature Switzerland.

Dong, Y., Sun, Y., and Tang, Z. (2013). Interactive visualization of 3d lunar model with texture and labels, using chang'e-1 data. *Science China Physics, Mechanics and Astronomy*, 56(10):2002–2008.

Dykes, T., Hassan, A., Gheller, C., Croton, D., and Krokos, M. (2018). Interactive 3d visualization for theoretical virtual observatories. *Monthly Notices of the Royal Astronomical Society*, 477(2):1495–1507.

Fazel Hesar, F., Raouf, M., Soltani, P., Foing, B., de Dood, M. J. A., and Verbeek, F. J. (2025). Using machine learning for lunar mineralogy-i: Hyperspectral imaging of volcanic samples. *Universe*, 11(4).

Flatken, M., Schneegans, S., Fellegara, R., and Gerndt, A. (2024). Immersive and interactive 3d visualization of large-scale geoscientific data. *PRESENCE: Virtual and Augmented Reality*, 33:57–76.

Fotopoulou, S. (2024). A review of unsupervised learning in astronomy. *Astronomy and Computing*, 48:100851.

Garcia, A. D., Schlueter, J., and Paddock, E. (2020). Training astronauts using hardware-in-the-loop simulations and virtual reality. In *AIAA Scitech 2020 Forum*, page 0167.

Génot, V., Beigbeder, L., Popescu, D., Dufourg, N., Gangloff, M., Bouchemit, M., Caussarieu, S., Toniutti, J.-P., Durand, J., Modolo, R., et al. (2018). Science data visualization in planetary and heliospheric contexts with 3dview. *Planetary and Space Science*, 150:111–130.

Gerloni, I. G., Carchiolo, V., Vitello, F. R., Sciacca, E., Becciani, U., Costa, A., Riggi, S., Bonali, F. L., Russo, E., Fallati, L., Marchese, F., and Tibaldi, A. (2018). Immersive virtual reality for earth sciences. In *2018 Federated Conference on Computer Science and Information Systems (FedCSIS)*, pages 527–534.

Gold, L., Bahremand, A., Richards, C., Hertzberg, J., Sese, K., Gonzalez, A., Purcell, Z., Powell, K., and LiKamWa, R. (2021). Visualizing planetary spectroscopy through immersive on-site rendering. In *2021 IEEE Virtual Reality and 3D User Interfaces (VR)*, pages 428–437.

Gold, T. (1955). The lunar surface. *Monthly Notices of the Royal Astronomical Society*, 115(6):585–604.

Grier, J. A., McEwen, A. S., Lucey, P. G., Milazzo, M., and Strom, R. G. (2001). Optical maturity of ejecta from large rayed lunar craters. *Journal of Geophysical Research: Planets*, 106(E12):32847–32862.

Hapke, B. (2001). Space weathering from mercury to the asteroid belt. *Journal of Geophysical Research: Planets*, 106(E5):10039–10073.

Hassan, A. and Fluke, C. J. (2011). Scientific visualization in astronomy: Towards the petascale astronomy era. *Publications of the Astronomical Society of Australia*, 28(2):150–170.

Helz, R., Cottrell, E., Brounce, M., and Kelley, K. (2017). Olivine-melt relationships and syneruptive redox variations in the 1959 eruption of kīlauea volcano as revealed by xanes. *Journal of Volcanology and Geothermal Research*, 333-334:1–14.

Isaacson, P. J., Pieters, C. M., Besse, S., Clark, R. N., Head, J. W., Klima, R. L., Mustard, J. F., Petro, N. E., Staid, M. I., Sunshine, J. M., et al. (2011). Remote compositional analysis of lunar olivine-rich lithologies with moon mineralogy mapper (m3) spectra. *Journal of Geophysical Research: Planets*, 116(E6).

Kodikara, G. R. and McHenry, L. J. (2020). Machine learning approaches for classifying lunar soils. *Icarus*, 345:113719.

König, B., Neukum, G., and Fechtig, H. (1977). Recent lunar cratering: Absolute ages of kepler, aristarchus, tycho. In *Lunar and Planetary Science VIII*, pages 555–557, Houston, TX. Lunar and Planetary Institute. ADS bibcode: 1977LPI.....8..555K.

Kuhail, M. A., Abdulkerim, A. Z., Thornquist, E., and Haile, S. Y. (2025). A review on the use of immersive technology in space research. *Telematics and Informatics Reports*, 17:100191.

Lan, F., Young, M., Anderson, L., Ynnerman, A., Bock, A., Borkin, M. A., Forbes, A. G., Kollmeier, J. A., and Wang, B. (2021). Visualization in astrophysics: Developing new methods, discovering our universe, and educating the earth. In *Computer graphics forum*, volume 40, pages 635–663. Wiley Online Library.

Le Mouélic, S., Langevin, Y., Erard, S., Pinet, P., Chevrel, S., and Daydou, Y. (2000). Discrimination between maturity and composition of lunar soils from integrated clementine uv-visible/near-infrared data: Application to the aristarchus plateau. *Journal of Geophysical Research: Planets*, 105(E4):9445–9455.

Lemelin, M., Lucey, P. G., Gaddis, L. R., Hare, T., and Ohtake, M. (2016). Global map products from the kaguya multiband imager at 512 ppd: Minerals, feo, and omat. In *47th Lunar and Planetary Science Conference (2016)*, page 2994. Abstract / extended abstract, USRA / LPSC.

Lin, C.-R., Loffin, R. B., and Stark, T. (1998). Virtual reality for geosciences visualization. In *Proceedings. 3rd asia pacific computer human interaction (cat. no. 98ex110)*, pages 196–201. IEEE.

Lin, C.-R. and Loftin, R. B. (1998). Application of virtual reality in the interpretation of geoscience data. In *Proceedings of the ACM symposium on Virtual reality software and technology*, pages 187–194.

Liu, F., Yang, R., Zhang, Y., Qiao, L., Wang, S., Yang, Y., and Wang, X. (2011). Distribution of olivine and pyroxene derived from clementine data in crater copernicus. *Journal of Earth Science*, 22(5):586–594.

Liu, H., Wang, Y., Wen, S., Zhang, S., Zhu, K., and Liu, J. (2025). Comprehensive evaluation of the lunar south pole landing sites using self-organizing maps for scientific and engineering purposes. *Remote Sensing*, 17(9):1579.

Lucey, P. G., Blewett, D. T., Taylor, G. J., and Hawke, B. R. (2000). Imaging of lunar surface maturity. *Journal of Geophysical Research: Planets*, 105(E8):20377–20386.

Lucey, P. G., Hawke, B. R., Pieters, C. M., Head, J. W., McCord, T. B., et al. (1986). A compositional study of the aristarchus region of the moon using near-infrared reflectance spectroscopy. *Journal of Geophysical Research*, 91(B4):344–354.

McKay, D. S., Heiken, G., Basu, A., Blanford, G., Simon, S., Reedy, R., French, B. M., and Papike, J. (1991). Lunar sourcebook: a user's guide to the moon. *The Lunar Regolith*, pages 285–356.

Mustard, J. F., Pieters, C. M., Isaacson, P. J., Head, J. W., Besse, S., Clark, R. N., Klima, R. L., Petro, N. E., Staid, M. I., Sunshine, J. M., et al. (2011). Compositional diversity and geologic insights of the aristarchus crater from moon mineralogy mapper data. *Journal of Geophysical Research: Planets*, 116(E6).

National Research Council (2007). *The Scientific Context for Exploration of the Moon*. The National Academies Press, Washington, DC.

Ohtake, M., Pieters, C., Isaacson, P., Besse, S., Yokota, Y., Matsunaga, T., Boardman, J., Yamomoto, S., Haruyama, J., Staid, M., Mall, U., and Green, R. (2013). One moon, many measurements 3: Spectral reflectance. *Icarus*, 226(1):364–374.

Olbrich, M., Graf, H., Keil, J., Gad, R., Bamfaste, S., and Nicolini, F. (2018). Virtual reality based space operations – a study of esa's potential for vr based training and simulation. In Chen, J. Y. and Fragomeni, G., editors, *Virtual, Augmented and Mixed Reality: Interaction, Navigation, Visualization, Embodiment, and Simulation*, pages 438–451, Cham. Springer International Publishing.

Peña-Asensio, E., Neira-Acosta, Á.-S., and Sánchez-Lozano, J. M. (2025). Evaluating potential landing sites for the artemis iii mission using a multi-criteria decision making approach. *Acta Astronautica*, 226:469–478.

Punzo, D., Van der Hulst, J., Roerdink, J. B., Oosterloo, T. A., Ramatsoku, M., and Verheijen, M. A. (2015). The role of 3-d interactive visualization in blind surveys of h i in galaxies. *Astronomy and Computing*, 12:86–99.

Sharp, J., Kelson, J., South, D., Saliba, A., and Kabir, M. A. (2025). Virtual reality and artificial intelligence as psychological countermeasures in space and other isolated and confined environments: A scoping review. *Acta Astronautica*.

Shishkina, T., Anosova, M., Migdisova, N., Portnyagin, M. V., Sushchevskaya, N., and Batanova, V. (2023). Trace elements in olivine of volcanic rocks: application to the study of magmatic systems. *Geochemistry International*, 61(1):1–23.

Shkuratov, Y., Surkov, Y., Ivanov, M., Korokhin, V., Kaydash, V., Videen, G., Pieters, C., and Stankevich, D. (2019). Improved chandrayaan-1 m3 data: A northwest portion of the aristarchus plateau and contiguous maria. *Icarus*, 321:34–49.

Shneiderman, B. (1996). The eyes have it: a task by data type taxonomy for information visualizations. In *Proceedings 1996 IEEE Symposium on Visual Languages*, pages 336–343.

Su, B., Yuan, J., Chen, Y., Yang, W., Mitchell, R. N., Hui, H., Wang, H., Tian, H., Li, X.-H., and Wu, F.-Y. (2022). Fusible mantle cumulates trigger young mare volcanism on the cooling moon. *Science Advances*, 8(42):eabn2103.

Sunshine, J. M. and Pieters, C. M. (1998). Determining the composition of olivine from reflectance spectroscopy. *Journal of Geophysical Research: Planets*, 103(E6):13675–13688.

Surkov, Y., Mall, U., and Korokhin, V. (2025). High resolution olivine abundance mapping in the copernicus crater combining spectral data of chandrayaan-1 m3 and kaguya mi. *Planetary and Space Science*, 256:106039.

Thapa, J., Sur, K., Chauhan, M., Ghosh, B., Kundu, A., Pundir, E., Verma, V. K., and Chauhan, P. (2025). Deciphering mineralogical and compositional variations in lunar basin, mare fecunditatis: An in-depth analysis using hyperspectral remote sensing techniques. *Advances in Space Research*, 75(4):4080–4098.

Thesniya, P., Rajesh, V., and Flahaut, J. (2020). Ages and chemistry of mare basaltic units in the grimaldi basin on the nearside of the moon: Implications for the volcanic history of the basin.

Thoresen, F., Drozdovskiy, I., Cowley, A., Laban, M., Besse, S., and Blunier, S. (2024). Insights into lunar mineralogy: An unsupervised approach for clustering of the moon mineral mapper (m3) spectral data. *arXiv preprint arXiv:2411.03186*.

Ting, L. and Wei, L. (2021). The application of immersive virtual reality technology in geoscience. *JUSTC*, 51(6):431–440.

Vapnik, V., Golowich, S., and Smola, A. (1996). Support vector method for function approximation, regression estimation and signal processing. *Advances in neural information processing systems*, 9.

Wallace, P. J., Plank, T., Bodnar, R. J., Gaetani, G. A., and Shea, T. (2021). Olivine-hosted melt inclusions: A microscopic perspective on a complex magmatic world. *Annual Review of Earth and Planetary Sciences*, 49(1):465–494.

Weller, R., Schröder, C., Teuber, J., Dittmann, P., and Zachmann, G. (2021). Vr-interactions for planning planetary swarm exploration missions in vamex-vtb. In *2021 IEEE Aerospace Conference (50100). IEEE*, pages 1–11.

Wu, Y. and Hapke, B. (2018). Spectroscopic observations of the moon at the lunar surface. *Earth and Planetary Science Letters*, 484:145–153.

Yamamoto, S., Nakamura, R., Matsunaga, T., Ogawa, Y., Ishihara, Y., Morota, T., Hirata, N., Ohtake, M., Hiroi, T., Yokota, Y., et al. (2010). Possible mantle origin of olivine around lunar impact basins detected by selene. *Nature Geoscience*, 3(8):533–536.

Zanetti, M., Hiesinger, H., van der Bogert, C., Reiss, D., Jolliff, B., et al. (2011a). Aristarchus crater: Mapping of impact melt and absolute age determination. In *42nd Lunar and Planetary Science Conference*, pages 7–11. The Woodlands, Texas.

Zanetti, M., van der Bogert, C., Reiss, D., and Hiesinger, H. (2011b). The lunar crater aristarchus: morphologic observations of impact melt features and absolute model age determination. *Eur Planet Sci*, 6:573.

Zhao, J., Wallgrün, J. O., LaFemina, P. C., Normandeau, J., and Klippel, A. (2019). Harnessing the power of immersive virtual reality - visualization and analysis of 3d earth science data sets. *Geo-spatial Information Science*, 22(4):237–250.

Zongyu, Y., Hongjie, X., Kaichang, D., and Ziyuan, O. (2012). Mapping lunar olivine using clementine spectral indices and chemical composition parameters. *Acta Geologica Sinica-English Edition*, 86(1):65–72.